Chapter I

Diluted magnetic semiconductor quantum dots

I.1 II-VI semiconductor quantum dots

I.1.1 Band structure of CdTe/ZnTe

ZnTe and CdTe are two II-VI semiconductor, meaning they are composed of an anion from the column VI of periodic table (Te), and a cation from the column II (Cd and Zn). They both crystallize as zinc blend when grown in Molecular Beam Epitaxy. As shown in Fig. I.1, in this structure, each species is organized in a face centred lattice, one them being shift from the other by a quarter of the [111] diagonal. Each ion is then in a tetragonal environment, meaning the zinc-blende structure is of the T_d space-group.

The external orbital of the cation are s for the cation ($4d^{10}5s^2$ for Cd, $3d^{10}4s^2$ for Zn) and p for the anion ($4d^{10}5s^25p^4$ for Te). Considering a N unit crystal, it then contain 8N valence electron, coming from the s and p levels of the ions. The s and p orbital of these atoms hybridize to form 8 levels, 4 bonding and 4 anti-bonding.

The lowest band of the bonding levels, coming from s orbitals, will be filled by 2N valence electron. 6N will be taken to fill the three higher energy bonding band, formed by the hybridization of p orbitals. Those bonding states form the valence band. At higher energy, the anti-bonding states form the conduction band. Since all the electron available are used to fill the valence band, the conduction band is empty in the ground state. The lower energy band of the conduction band are formed by the anti-symmetric combination of the s orbitals. At higher energy, the anti-symmetric hybridization of p orbitals form three other bands.

Introducing the spin-orbit interaction, the conduction band, formed by the hybridazation of s orbitals, is of Γ_6 (spherical) symmetry at the center of the

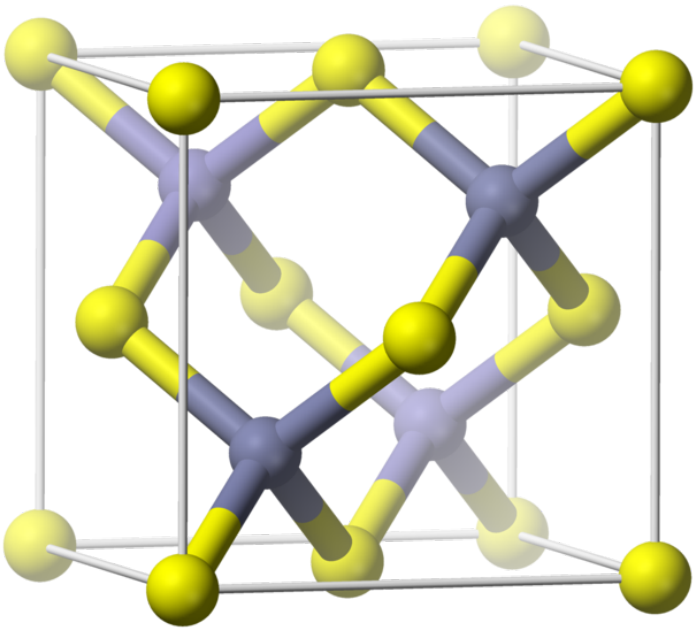

Figure I.1: Zinc-blende crystal structure and first Brillouin zone.

Brillouin zone, two-fold degenerated, with an orbital momentum (spin) $\sigma = 1/2$. In a similar fashion, the valence band will be split into to band: a first one of Γ_8 symmetry, with a spin $J = 3/2$, four-fold degenerated ; and the second one, at lower energy, of Γ_7 symmetry, with a spin 1/2, two-fold degenerated. The splitting $\Gamma_7 - \Gamma_8$ is of $\Delta_{SO} \simeq 0.9$ eV in II-VI semiconductor.

The whole CdTe band structure is presented on Fig. I.2. One can note that CdTe is a direct gap semiconductor: the highest energy point of the valence band correspond to the lowest energy point of the conduction band, in Γ. As we move away from this point, the valence band into two branches: one with small curvature, meaning a high effective mass for the carriers on it, is called the heavy-hole (hh) band, while the one presenting the highest curvature and smallest effective mass is called the light-hole (lh) band.

One way to understand this evolution is to apply the **k.p** approximation, as proposed by Kane in 1957 [1]. This model gives an estimation of the electronic band structure starting from the exact solution and energy of the Schrödinger equation at the center of the Brillouin. The hamiltonian to resolve is then :

$$\left(\frac{p^2}{2m_0} + U(\mathbf{r})\right)\psi_{n,\mathbf{k}} = E_{n,\mathbf{k}}\psi_{n,\mathbf{k}} \tag{I.1}$$

Figure I.2: CdTe/ZnTe band structures

with $U(\mathbf{r})$ the potential of the crystal and $\psi_{n,\mathbf{k}}$ the Bloch wave, separated between a periodic part $u_{n,\mathbf{k}}(\mathbf{r})$ and plane-wave part $e^{i\mathbf{k}.\mathbf{r}}$ as follow :

$$\psi_{n,\mathbf{k}} = u_{n,\mathbf{k}}(\mathbf{r})e^{i\mathbf{k}.\mathbf{r}} \tag{I.2}$$

Neglecting the Γ_7 band at lower energy, we solve this hamiltonian for carrier on the Γ_6 and Γ_8 bands [2]. The z-axis is defined along the growth direction of the semiconductor and chosen as the quantization axis. We then find the energy:

$$\begin{aligned} E_c(k_z) &= E_c + \frac{\hbar^2 k_z^2}{2m_c} \\ E_{v,\pm\frac{1}{2}}(k_z) &= E_v - \frac{\hbar^2 k_z^2}{2m_{lh}} \\ E_{v,\pm\frac{3}{2}}(k_z) &= E_v + \frac{\hbar^2 k_z^2}{2m_0} \end{aligned} \tag{I.3}$$

with E_c (E_v) the energy of the conduction band (respectively, the valence band), m_c the effective mass of the carrier on the conduction and m_{lh} the effective mass of the light hole. One can see that the splitting of the valence band separate the carrier with a spin $J_z = \pm\frac{3}{2}$ (hh) from the one with a spin $J_z = \pm\frac{1}{2}$ (lh). However, the neglecting of the bands other than Γ_6 and Γ_8 lead to a positive curvature for the hh. To correct this problem, we would have to take into account higher energy conduction band, which will repel the hh band and give it its negative curvature.

Another solution to have the matrix describing the Γ_8 band is to use symmetry consideration. Luttinger showed in 1956 [3] that the only Hamiltonian fulfilling

the cubic symmetry is:

$$\mathcal{H}_L = -\frac{h^2}{2m_0}\left(\gamma_1 k^2 I_4 - 2\gamma_2 \sum_i k_i^2 \left(J_i^2 - \frac{1}{3}J^2\right) - 2\gamma_3(k_x k_y(J_x J_y + J_y J_x) + c.p.)\right) \tag{I.4}$$

with γ_1, γ_2 and γ_3 the Luttinger parameters, I_4 the 4×4 identity matrix, $\mathbf{k}$ a vector of the Brillouin zone, $\mathbf{J}$ the orbital momentum operator with J_x, J_y and J_z being 4×4 matric satisfying $[J_x, J_y] = iJ_z$ and circular permutation, and $c.p$ standing for "circular permutation". This hamiltonian can be simplified using the parameters:

$$\begin{aligned} A &= \gamma_1 + \tfrac{5}{2}\gamma_2 \\ B &= 2\gamma_2 \\ C &= 2(\gamma_3 - \gamma_2) \end{aligned} \tag{I.5}$$

Using these, the Luttinger hamiltonian can be rewritten:

$$\mathcal{H}_L = -\frac{h^2}{2m_0}(Ak^2 I_4 - B(\mathbf{k}.\mathbf{J})^2 + C(k_x k_y(J_x J_y + J_y J_x) + c.p.)) \tag{I.6}$$

The B-term lift the degeneracy of the Γ_8 band into two sub-bands as shown above, and is invariant under arbitrary rotations. The C-term describes the warping of the valence band.

In the spherical approximation, the Luttinger hamiltonian has two eigenvalues:

$$\begin{aligned} E_{hh} &= -\frac{\hbar^2 k^2}{2m_0(A-2.25B)^{-1}} = -\frac{\hbar^2 k^2}{2m_0(\gamma_1-2\gamma_2)^{-1}} = -\frac{\hbar^2 k^2}{2m_{hh}} \\ E_{lh} &= -\frac{\hbar^2 k^2}{2m_0(A-0.25B)^{-1}} = -\frac{\hbar^2 k^2}{2m_0(\gamma_1+2\gamma_2)^{-1}} = -\frac{\hbar^2 k^2}{2m_{lh}} \end{aligned} \tag{I.7}$$

We find back the value of the effective mass for the lh, along with a value for the hh. The hh band also presents here a negative curvature, as expected.

The parameters and carriers effective masses are given in the Tab. I.1.1.

I.1.2 Lattice mismatch and the Bir-Pikus Hamiltonian

ZnTe crystal has a lattice parameter of a_{ZnTe} =6.10 Å, while CdTe one is of a_{CdTe} =6.48 Å. This lattice mismatch results in stress in a CdTe layer grown on a ZnTe substrate:

$$\epsilon_\perp = \frac{a_{ZnTe} - a_{CdTe}}{a_{CdTe}} = -5.8\% \tag{I.8}$$

In order to represent this strain and see their effect on the band, especially the Γ_8 band, we need to define a hamiltonian representing them. These strains deform

	CdTe	ZnTe
E_g	1606 meV	2391 meV
ϵ_r	10.6	9.7
a_0	6.48 Å	6.10 Å
Δ_{SO}	0.90 eV	0.91 eV
γ_1	4.8	4.07
γ_2	1.5	0.78
γ_3	1.9	1.59
$m_{hh,z}$	0.556	0.398
$m_{hh,\perp}$	0.159	0.206
$m_{lh,z}$	0.128	0.178
$m_{lh,\perp}$	0.303	0.303
m_e	0.096	0.116

Table I.1: Physical parameters for CdTe and ZnTe.

the structure, so let's begin the representation with an volume $V = (x\mathbf{u_x} + y\mathbf{u_y} + z\mathbf{u_z}$, with $(\mathbf{u_x}, \mathbf{u_y}, \mathbf{u_z})$ an ortho-normalized basis. This volume will transform into another one $V' = (x\mathbf{u'_x} + y\mathbf{u'_y} + z\mathbf{u'_z})$, where:

$$\begin{aligned} \mathbf{u'_x} &= (1+\epsilon'_{xx})\mathbf{u_x} + \epsilon'_{xy}\mathbf{u_y} + \epsilon'_{xz}\mathbf{u_z} \\ \mathbf{u'_y} &= \epsilon'_{yx}\mathbf{u_x} + (1+\epsilon'_{yy})\mathbf{u_y} + \epsilon'_{yz}\mathbf{u_z} \\ \mathbf{u'_z} &= \epsilon'_{zx}\mathbf{u_x} + \epsilon'_{zy}\mathbf{u_y} + (1+\epsilon'_{zz})\mathbf{u_z} \end{aligned} \tag{I.9}$$

ϵ'_{ij} represents an expansion of the vector i in the direction j. They are small deformation of the lattice, so we choose $|\epsilon'_{ij}| \ll 1$. Such transformations can be decomposed in a symmetric part and an antisymetric one. We note $\overline{\overline{\epsilon}}$ the symmetric part, called the strain tensor, defined such as:

$$\epsilon_{ii} = \epsilon'_{ii} \tag{I.10}$$

$$\epsilon_{ij} = \frac{1}{2}\left(\epsilon'_{ij} + \epsilon'_{ji}\right) \tag{I.11}$$

In the linear regime, the strain tensor $\overline{\overline{\epsilon}}$ is proportional to the stress tensor $\overline{\overline{\sigma}}$, where σ_{ij} describe a force parallel to i applied on a surface perpendicular to j. Therefore, σ_{ii} will describe an elongation or compression stress, while σ_{ij} $(i \neq j)$ represents a shear stress. Since these tensor are symmetric, we can reduce the number of coefficient from nine to six: σ_{xx}, σ_{yy}, σ_{zz}, $\sigma_{xy} = \sigma_{yx}$, $\sigma_{xz} = \sigma_{zx}$ and

$\sigma_{yz} = \sigma_{zy}$. Therefore, in the linear regime and for a cubic crystal, we can write the Hooke's law:

$$\begin{bmatrix} \sigma_{xx} \\ \sigma_{yy} \\ \sigma_{zz} \\ \sigma_{xy} \\ \sigma_{xz} \\ \sigma_{yz} \end{bmatrix} = \begin{bmatrix} C_{11} & C_{12} & C_{12} & 0 & 0 & 0 \\ C_{12} & C_{11} & C_{12} & 0 & 0 & 0 \\ C_{12} & C_{12} & C_{11} & 0 & 0 & 0 \\ 0 & 0 & 0 & 2C_{44} & 0 & 0 \\ 0 & 0 & 0 & 0 & 2C_{44} & 0 \\ 0 & 0 & 0 & 0 & 0 & 2C_{44} \end{bmatrix} \begin{bmatrix} \epsilon_{xx} \\ \epsilon_{yy} \\ \epsilon_{zz} \\ \epsilon_{xy} \\ \epsilon_{xz} \\ \epsilon_{yz} \end{bmatrix} \tag{I.12}$$

Since x, y and z are physically equivalent, as well as xy, xz and yz, only two diagonal coefficient are needed, C_{11} and C_{44}. These coefficient coupling strains in a direction to a force in the same direction are obviously positives.

When the considered cube is compressed in one direction (e.g. $\epsilon_{zz} < 0$), it will expand in the other direction in order to minimize elastic energy (ϵ_{xx}, $\epsilon_{yy} > 0$ in the example). If we don't allow strain in these other directions ($\epsilon_{xx} = \epsilon_{yy} = 0$), a stress in the x and y directions had to be applied to keep the cube from expanding in these directions (σ_{xx}, $\sigma_{yy} < 0$ in the example). We can therefore physically expect $C_{12} > 0$.

The strain hamiltonian can be constructed noticing that the strain tensor $\bar{\bar{\epsilon}}$ induces a shift in the bands energy, and that any ϵ_{ij} has the same symmetry as $k_i k_j$. The hamiltonian should then be formarly identical to the Luttinger hamiltonian. In the Γ_8 subspace, we can then use the Luttinger Hamiltonian, written in Eq. I.4, replacing the $k_i k_j$ by ϵ_{ij}. We obtain the Bir-Pikus Hamiltonian by replacing the γ_j parameters by the Bir-Pikus parameters a_ν, b_ν and d_ν [4]:

$$\mathcal{H}_{BP} = a_\nu \epsilon I_4 + b_\nu \sum_i \epsilon_{ii} \left(J_i^2 - \frac{1}{3} J^2 \right) + \frac{d_\nu}{\sqrt{3}} (\epsilon_{xy}(J_x J_y + J_y J_x) + c.p) \tag{I.13}$$

with $\epsilon = Tr(\bar{\bar{\epsilon}}) = \epsilon_{xx} + \epsilon_{yy} + \epsilon_{zz}$.

The a_ν term, called the hydrostatic term, is to shift the Γ_8 energy. The b_ν term represents the shear strain. In case of non-equal ϵ_{ii}, its effect is to lift up the two Γ_8 sub-bands as did a $k \neq 0$ in the Luttinger hamiltonian. The d_ν term, the pure shear strain (i.e ϵ_{ij} with $i \neq j$), has the same effect on the Γ_8 band.

One can notice that the Bir-Pikus hamiltonian is completely independant from $\mathbf{k}$, meaning that the band hamiltonian of a strain semiconductor is simply the sum of the sum of the Luttinger hamiltonian $\mathcal{H}_L$ (Eq. I.4) and the Bir-Pikus hamiltonian $\mathcal{H}_{BP}$ (Eq. I.13).

Let see how this apply to a CdTe layer deposited on a ZnTe layer. We define z as the growth direction. As shown at the begin of this part, CdTe and ZnTe have a lattice mismatch of 5.8%. Since both crystallize in a cubic lattice, the strain is

the same in the x and y direction. We can then write the strain in the xy plane:

$$\epsilon_{xx} = \epsilon_{yy} = \epsilon_{\perp} = \frac{a_{ZnTe} - a_{CdTe}}{a_{CdTe}} \tag{I.14}$$

In the z direction, however, no stress apply: the crystal is free to expand in this direction in order to reduce the elastic energy. Therefore, we can write $\sigma_{zz} = 0$ and, according to Hooke's law in Eq. I.12:

$$\begin{aligned} \sigma_{zz} &= C_{12}\epsilon_{xx} + C_{12}\epsilon_{yy} + C_{11}\epsilon_{zz} \\ &= 0 \end{aligned} \tag{I.15}$$

Using equality I.14, we can then deduce:

$$\epsilon_{zz} = -\frac{2C_{12}}{C_{11}}\epsilon_{\perp} = -\frac{2C_{12}}{C_{11}}\frac{a_{ZnTe} - a_{CdTe}}{a_{CdTe}} \tag{I.16}$$

Since we grow CdTe over a ZnTe substrate, the CdTe lattice is compressed in the plane, i.e. $\epsilon_{\perp} < 0$. Since C_{11}, $C_{12} > 0$ and $\epsilon_{\perp} < 0$ for CdTe over ZnTe (see Eq. I.14, one can easily deduce that $\epsilon_{zz} > 0$. In the hypothesis of no defect created by the lattice mismatch, all the other strain terms are equal to zero. We can then decompose this strain into two component: a hydrostatic part describing the volume variation without breaking the cubic symmetry, and a shear part introducing an anisotropy, breaking this symmetry:

$$\overline{\overline{\epsilon_{hyd}}} = \frac{1}{3}(\epsilon_{xx} + \epsilon_{yy} + \epsilon_{zz})I_3 \tag{I.17}$$

$$\overline{\overline{\epsilon_{sh}}} = \bar{\bar{\epsilon}} - \overline{\overline{\epsilon_{hyd}}} \tag{I.18}$$

One can notice that $Tr(\overline{\overline{\epsilon_{hybd}}}) = Tr(\bar{\bar{\epsilon}}) = \epsilon$. Since in the case of a hydrostatic compression, such as what is the case with CdTe over ZnTe, $\epsilon_{hybd} < 0$, we then have $\epsilon < 0$ and, according to the Bir-Pikus hamiltonian (Eq. I.13), the gap of CdTe increase. For CdTe, Bir-Pikus parameter are $a_\nu = 0.91$ eV, $b_\nu = 0.99$ eV and $d_\nu = 2.76$ eV [5].

Seeing that $\epsilon_{ij} = 0$ for $i \neq j$, we can rewrite the Bir-Pikus hamiltonian without the shear strain term. Moreover, since $J^2 = J_x^2 + J_y^2 + J_z^2$ and that $\epsilon_{xx} = \epsilon_{yy} = \epsilon_{\perp}$, we can simplify this hamiltonian to:

$$\mathcal{H}_{BP,biax} = a_\nu \epsilon I_4 + \frac{b_\nu}{3}(\epsilon_{\perp} - \epsilon_{zz})(J_x^2 + J_y^2 - 2J_z^2) \tag{I.19}$$

And, since we are in the valence band with $J = \frac{3}{2}$ and $J_x^2 + J_y^2 + J_z^2 = J(J+1)I_4$, we can simplify the Bir-Pikus hamiltonian to its final form in the case of biaxal strain:

$$\mathcal{H}_{BP,biax} = \left(a_\nu \epsilon + \frac{5}{4} b_\nu(\epsilon_\nu - \epsilon_{zz})\right) I_4 - b_\nu(\epsilon_\nu - \epsilon_{zz})J_z^2 \tag{I.20}$$

Using Eq. I.14 and I.16, we can easily calculate $\epsilon_\perp - \epsilon_z$. Since $J_z|n\rangle = n|n\rangle$, we find:

$$\begin{aligned} E_{\pm\frac{3}{2}} - E_{\pm\frac{1}{2}} &= -2b_\nu \left(1 + \frac{2C_{12}}{C_{11}}\right) \frac{a_{ZnTe} - a_{CdTe}}{a_{CdTe}} \\ &= 2b_\nu \left(1 + \frac{2C_{12}}{C_{11}}\right) \frac{a_{CdTe} - a_{ZnTe}}{a_{CdTe}} \end{aligned} \tag{I.21}$$

We find that, in a fully strained CdTe layer over a ZnTe substrate, the hh band is 300 meV above the lh one. In first approximation, we can then neglect the lh contribution in these nanostructures.

I.1.3 3D confinement: the quantum dot

Embedding a semiconductor in another one of larger creates trap for carrier, confining them in one or multiple. CdTe conduction band (resp. valence band) is a lower (resp. higher) energy than ZnTe ones, creating such a trap. Using the procedure described in Chap. **??**, we can create nanometre size island of CdTe in a ZnTe lattice, effectively confining electron in all three direction, acting like an 3D well for the free carriers. This confinement lead to a quantization of the carriers energy level and a discretization of the optical properties. This confinement being analogue to the Coulomb interaction of an isolated atom, such a structure is often dubbed "artificial atom". However, the interaction between the hole and the electron cannot be overlook, adding Coulomb interaction between the particule and the quasi-particule. It consists of an attractive term, shifting energy levels, and an exchange interaction (discussed in Chap. I.2.4). Moreover, the hole being the absence of an electron, its energy, charge, spin, orbital momentum, $\mathbf{k}$ and mass are, by definition, opposite to the missing electron. The electron-hole system has a hydrogen-like behaviour and is called an exciton.

Before going to the exchange part, we will see the optical properties of this system. In order to do so, we develop the carrier wave-function on the Bloch states:

$$\Psi(\mathbf{r}) = \sum_{n,k} c_{n,k} u_{n,k}(\mathbf{r}) e^{i\mathbf{k}.\mathbf{r}} \tag{I.22}$$

Since we are in a confined environment, we can only consider the states around $\mathbf{k} = 0$. Since we consider the band extrema, we neglect the inter-band wave function mixing in a first time and use the effective-mass approximation. We can then limit the expansion of Bloch state to an expansion on the $u_{n,0}(\mathbf{r})e^{i\mathbf{k}.\mathbf{r}}$, with

Figure I.3: Dots STM images

$n = \Gamma_6$ for the conduction band and $n = \Gamma_8$ for the valence. We can then write:

$$\Psi_c(\mathbf{r}) \simeq \sum_k c_k u_{\Gamma_6,0}(\mathbf{r}) e^{i\mathbf{k}.\mathbf{r}} = F_e(\mathbf{r}) u_{\Gamma_6,0} \tag{I.23}$$

$$\Psi_v(\mathbf{r}) \simeq \sum_{J_z=\{\pm\frac{3}{2},\pm\frac{1}{2}\},k} c_{J_z,k} u_{\Gamma_8,J_z}(\mathbf{r}) e^{i\mathbf{k}.\mathbf{r}} = \sum_{J_z=\{\pm\frac{3}{2},\pm\frac{1}{2}\}} F_{J_z}(\mathbf{r}) u_{\Gamma_8,J_z} \tag{I.24}$$

with $F_e(\mathbf{r}) = \sum_{n,k} c_k e^{i\mathbf{k}.\mathbf{r}}$ the electron envelop function and $F_{J_z}(\mathbf{r}) = c_{J_z,k} e^{i\mathbf{k}.\mathbf{r}}$, $J_z = \{\pm\frac{3}{2}, \pm\frac{1}{2}\}$ the hole envelop functions.

The effective mass approximation allow us to replace the periodic crystal potential and the free-electron kinetic energy by the effective Hamiltonian representing the band extrema, using m_e for the conduction band and $\mathcal{H}_L + \mathcal{H}_{BP}$ for the top of the valence band. Considering the effective mass is the same in CdTe and ZnTe, we can now work with the simple picture of an effective mass carrier with the envelop function defined in Eqs. I.23 and I.24, trapped in a potential $V_e(\mathbf{r})$ for the conduction band or $V_h(\mathbf{r})$ for the valence band, creating by the band offset between the two semiconductors. We write the Schrödinger equations for these particle:

$$\left(\frac{\hbar^2}{2m_e}\Delta\right) F_e(\mathbf{r}) + V_e(\mathbf{r}) F_e(\mathbf{r}) = E F_e(\mathbf{r}) \tag{I.25}$$

$$(\tilde{\mathcal{H}}_L + \tilde{\mathcal{H}}_{BP} + V_h(\mathbf{r})) \begin{pmatrix} F_{+\frac{3}{2}}(\mathbf{r}) \\ F_{+\frac{1}{2}}(\mathbf{r}) \\ F_{-\frac{1}{2}}(\mathbf{r}) \\ F_{-\frac{3}{2}}(\mathbf{r}) \end{pmatrix} = E \begin{pmatrix} F_{+\frac{3}{2}}(\mathbf{r}) \\ F_{+\frac{1}{2}}(\mathbf{r}) \\ F_{-\frac{1}{2}}(\mathbf{r}) \\ F_{-\frac{3}{2}}(\mathbf{r}) \end{pmatrix} \tag{I.26}$$

with $\tilde{\mathcal{H}}_L$ and $\tilde{\mathcal{H}}_{BP}$ the hole hamiltonians, opposite to the electron hamiltonians defined in Eq. I.4 and I.13. In $\tilde{\mathcal{H}}_L$, the k-terms transform into a gradient of the envelop function with the form $i\nabla$. For simplicity, the $\tilde{}$ will be dropped in the next equations. The derivation of the effective mass approximation can be found in reference [6].

In order to analytically solve these hamiltonian, another approximation is necessary. As discussed in section I.2, $\mathcal{H}_L$ couple the hh and lh through its non-diagonal terms, while $\mathcal{H}_{BP}$ lift their degeneracy, as shown in section I.1.2. Considering the presence of biaxial strain, we can neglect the non-diagonal terms of $\mathcal{H}_L$ in regard to the action of $\mathcal{H}_{BP}$. This is the heavy hole approximation, un coupling the four differential equations defined in Eq. I.26. Only the ground states $|\pm\frac{3}{2}\rangle$ are considered, with the effective mass given by the diagonal term of $\mathcal{H}_L$, noted $m_{h,\parallel}$ in the plane and $m_{h,z}$ along the growth axis.

In the general case, we still cannot solve this problem. However, it is however possible for some chosen potential. Let's consider a lens like quantum dot, with a radius in the xy plane, noted ρ, much larger than it height L_z. We can therefore define two different harmonic oscillator of potential: a 2D oscillator $V_{c,v}(\rho)$ in the plane, and a 1D oscillator $V_{c,v}(z)$ along the growth axis:

$$V_{c,v}(\rho) = 4\Delta E_{c,v}\frac{\rho^2}{L_z^2} \tag{I.27}$$

$$V_{c,v}(z) = 4\Delta E_{c,v}\frac{z^2}{L_z^2} \tag{I.28}$$

with $\Delta E_{c,v}$ the difference of conduction (resp. valence) band energy between the semiconductor. The potential of the whole quantum will the be $V_{c,v}(\mathbf{r}) = V_{c,v}(\rho) + V_{c,v}(z)$. Separating the potential in those two parts means we are searching for solution of the form $F(z,\rho,\theta) = \chi(z)\phi_{n,m}(\rho,\theta)$, with θ the angle between the position vector and the x axis.

We write the characteristic spatial width and characteristic frequency of the 2D harmonic oscillator felt by the hole:

$$\Sigma_\rho^h = \sqrt{\frac{\hbar}{m_{h,\parallel}\omega_\rho^h}} \tag{I.29}$$

$$\omega_\rho^h = \sqrt{\frac{8\Delta E_v}{m_{h,\parallel}L_\rho^2}} \tag{I.30}$$

We can write the same equality along z replacing ρ by z and $m_{h,\parallel}$ by $m_{h,z}$. The same can be done for electron, replacing the $m_{h,\parallel}$ or $m_{h,z}$ by m_e and E_v by E_c.

We can find in textbook such as ref. [7] the solution of a harmonic oscillator from which we can deduce the solution for the ground state (GS) and the first

two degenerated excited states. The first excited state is found to have an angular momentum $l_z = \pm 1$, and is then noted $Exc, \pm 1$. The envelop functions and energy are then found to be:

$$F_{c,v}^{GS}(z,\rho,\theta) = \frac{1}{(\sqrt{\pi}\Sigma_z)^{\frac{1}{2}}} \exp\left(-\frac{z^2}{2\Sigma_z^2}\right) \frac{1}{(\sqrt{\pi}\Sigma_\rho)^{\frac{1}{2}}} \exp\left(-\frac{\rho^2}{2\Sigma_\rho^2}\right) \tag{I.31}$$

$$E_{e,h}^{GS} = \hbar \frac{\omega_z^{e,h} + \omega_\rho^{e,h}}{2} \tag{I.32}$$

$$F_{c,v}^{Exc,\pm 1}(z,\rho,\theta) = \frac{1}{(\sqrt{\pi}\Sigma_z)^{\frac{1}{2}}} \exp\left(-\frac{z^2}{2\Sigma_z^2}\right) \frac{1}{(\sqrt{\pi}\Sigma_\rho)^{\frac{1}{2}}} \exp\left(-\frac{\rho^2}{2\Sigma_\rho^2}\right) \frac{\rho}{\sigma_\rho} e^{\pm i\theta} \tag{I.33}$$

$$E_{e,h}^{Exc,\pm 1} = \hbar \frac{\omega_z^{e,h} + 3\omega_\rho^{e,h}}{2} \tag{I.34}$$

We see that this energy level are quantified in a way looking like an isolated atom, as pointed earlier. In reference to the atomic notation, the ground state, lower energy level, is noted S and the two first degenerated level are noted P, even though atomic p-states usually are 3 fold degenerated.

One remarkable feature of the envelop functions is that both GS and the two first excited states present the same envelop along the z axis. The cause is directly the symmetry of the QD: since $L_z \ll L_\rho$, $\omega_z^{e,h} \gg \omega_\rho^{e,h}$, and since $E_{osc.\ harmo.} = (n + \frac{1}{2})\hbar\omega$, the next possible envelop function along the z axis is at higher energy than the next one in the plane. This geometry is also responsible for the 2 fold degeneracy of the P-states.

Both the GS and the excited states are once again degenerated due to the spin of the electron and the hole. The electron is in the conduction band with the Γ_6 symmetry: it can then take the value $\sigma_z = \pm\frac{1}{2}$ (noted $|\uparrow\rangle$ for $+\frac{1}{2}$ and $|\downarrow\rangle$ for $-\frac{1}{2}$). Since we are in the hh approximation, considering the lh are high enough energy to be negligible, the hole spin can only take the values $J_z = \pm\frac{3}{2}$ (noted $|\Uparrow\rangle$ for $+\frac{3}{2}$ and $|\Downarrow\rangle$ for $-\frac{3}{2}$). As pointed ahead, the hole is defined with the opposed characteristic of the missing electron (which may not be the one trapped in the QD). For example, a hole $|\Downarrow\rangle$ corresponds to the absence of a valence electron $\Psi_v(\mathbf{r}) = u_{\Gamma_8,\frac{3}{2}}(\mathbf{r}) F_{\frac{3}{2}}(\mathbf{r})$.

I.1.4 Valence band mixing

Lorem ipsum dolor sit amet, consectetur adipiscing elit. Curabitur tortor quam, imperdiet quis facilisis sed, fringilla a quam. Cras ante odio, hendrerit ac ante nec, cursus imperdiet urna. Mauris convallis ultricies purus, nec condimentum erat bibendum vel. Aliquam erat volutpat. Pellentesque condimentum, eros a

consequat accumsan, turpis sem euismod nisi, sed fringilla quam turpis sit amet erat. Mauris dictum odio sed nisi dapibus, et molestie mauris rutrum. Praesent convallis dolor in nibh blandit bibendum. Quisque sit amet arcu consectetur lorem luctus venenatis nec quis dui. Aliquam erat volutpat. Aenean auctor elit nec tristique dignissim. Nulla massa mi, efficitur semper ex id, pretium eleifend massa. Vivamus sit amet orci scelerisque, gravida est ut, vulputate odio.

Curabitur eget ipsum egestas dui viverra suscipit. Cras aliquet lacus vitae erat finibus semper. Nulla pharetra eget urna vitae sodales. Nunc faucibus velit lacus, nec ornare eros aliquet quis. Donec a orci nec sem pulvinar ultricies sit amet ut arcu. Nullam id vehicula enim, at tincidunt velit. Duis vestibulum lorem a molestie fringilla. Nullam tincidunt semper placerat. Donec nibh sem, ornare eget cursus ac, luctus sit amet eros. Phasellus eget interdum nisi. Donec mollis risus id lectus fringilla, et commodo risus iaculis. Donec at lacus sed nibh posuere posuere sit amet eget sapien. In dignissim, enim sit amet convallis fermentum, lacus nulla gravida tortor, non facilisis ex nisl sit amet augue. Maecenas eu enim condimentum, consectetur ligula vel, tincidunt nisl. Nam laoreet dictum volutpat. Donec at erat venenatis, ultrices lorem ac, vestibulum neque.

I.2 Exchange interaction between carrier and magnetic atom

I.2.1 Exchange interaction in Diluted Magnetic Semiconductors

Lorem ipsum dolor sit amet, consectetur adipiscing elit. Curabitur tortor quam, imperdiet quis facilisis sed, fringilla a quam. Cras ante odio, hendrerit ac ante nec, cursus imperdiet urna. Mauris convallis ultricies purus, nec condimentum erat bibendum vel. Aliquam erat volutpat. Pellentesque condimentum, eros a consequat accumsan, turpis sem euismod nisi, sed fringilla quam turpis sit amet erat. Mauris dictum odio sed nisi dapibus, et molestie mauris rutrum. Praesent convallis dolor in nibh blandit bibendum. Quisque sit amet arcu consectetur lorem luctus venenatis nec quis dui. Aliquam erat volutpat. Aenean auctor elit nec tristique dignissim. Nulla massa mi, efficitur semper ex id, pretium eleifend massa. Vivamus sit amet orci scelerisque, gravida est ut, vulputate odio.

Curabitur eget ipsum egestas dui viverra suscipit. Cras aliquet lacus vitae erat finibus semper. Nulla pharetra eget urna vitae sodales. Nunc faucibus velit lacus, nec ornare eros aliquet quis. Donec a orci nec sem pulvinar ultricies sit amet ut arcu. Nullam id vehicula enim, at tincidunt velit. Duis vestibulum lorem a molestie fringilla. Nullam tincidunt semper placerat. Donec nibh sem, ornare

eget cursus ac, luctus sit amet eros. Phasellus eget interdum nisi. Donec mollis risus id lectus fringilla, et commodo risus iaculis. Donec at lacus sed nibh posuere posuere sit amet eget sapien. In dignissim, enim sit amet convallis fermentum, lacus nulla gravida tortor, non facilisis ex nisl sit amet augue. Maecenas eu enim condimentum, consectetur ligula vel, tincidunt nisl. Nam laoreet dictum volutpat. Donec at erat venenatis, ultrices lorem ac, vestibulum neque.

I.2.2 Mn case

Lorem ipsum dolor sit amet, consectetur adipiscing elit. Curabitur tortor quam, imperdiet quis facilisis sed, fringilla a quam. Cras ante odio, hendrerit ac ante nec, cursus imperdiet urna. Mauris convallis ultricies purus, nec condimentum erat bibendum vel. Aliquam erat volutpat. Pellentesque condimentum, eros a consequat accumsan, turpis sem euismod nisi, sed fringilla quam turpis sit amet erat. Mauris dictum odio sed nisi dapibus, et molestie mauris rutrum. Praesent convallis dolor in nibh blandit bibendum. Quisque sit amet arcu consectetur lorem luctus venenatis nec quis dui. Aliquam erat volutpat. Aenean auctor elit nec tristique dignissim. Nulla massa mi, efficitur semper ex id, pretium eleifend massa. Vivamus sit amet orci scelerisque, gravida est ut, vulputate odio.

Curabitur eget ipsum egestas dui viverra suscipit. Cras aliquet lacus vitae erat finibus semper. Nulla pharetra eget urna vitae sodales. Nunc faucibus velit lacus, nec ornare eros aliquet quis. Donec a orci nec sem pulvinar ultricies sit amet ut arcu. Nullam id vehicula enim, at tincidunt velit. Duis vestibulum lorem a molestie fringilla. Nullam tincidunt semper placerat. Donec nibh sem, ornare eget cursus ac, luctus sit amet eros. Phasellus eget interdum nisi. Donec mollis risus id lectus fringilla, et commodo risus iaculis. Donec at lacus sed nibh posuere posuere sit amet eget sapien. In dignissim, enim sit amet convallis fermentum, lacus nulla gravida tortor, non facilisis ex nisl sit amet augue. Maecenas eu enim condimentum, consectetur ligula vel, tincidunt nisl. Nam laoreet dictum volutpat. Donec at erat venenatis, ultrices lorem ac, vestibulum neque.

I.2.3 Cr case

Lorem ipsum dolor sit amet, consectetur adipiscing elit. Curabitur tortor quam, imperdiet quis facilisis sed, fringilla a quam. Cras ante odio, hendrerit ac ante nec, cursus imperdiet urna. Mauris convallis ultricies purus, nec condimentum erat bibendum vel. Aliquam erat volutpat. Pellentesque condimentum, eros a consequat accumsan, turpis sem euismod nisi, sed fringilla quam turpis sit amet erat. Mauris dictum odio sed nisi dapibus, et molestie mauris rutrum. Praesent convallis dolor in nibh blandit bibendum. Quisque sit amet arcu consectetur lorem luctus venenatis nec quis dui. Aliquam erat volutpat. Aenean auctor elit nec

tristique dignissim. Nulla massa mi, efficitur semper ex id, pretium eleifend massa. Vivamus sit amet orci scelerisque, gravida est ut, vulputate odio.

Curabitur eget ipsum egestas dui viverra suscipit. Cras aliquet lacus vitae erat finibus semper. Nulla pharetra eget urna vitae sodales. Nunc faucibus velit lacus, nec ornare eros aliquet quis. Donec a orci nec sem pulvinar ultricies sit amet ut arcu. Nullam id vehicula enim, at tincidunt velit. Duis vestibulum lorem a molestie fringilla. Nullam tincidunt semper placerat. Donec nibh sem, ornare eget cursus ac, luctus sit amet eros. Phasellus eget interdum nisi. Donec mollis risus id lectus fringilla, et commodo risus iaculis. Donec at lacus sed nibh posuere posuere sit amet eget sapien. In dignissim, enim sit amet convallis fermentum, lacus nulla gravida tortor, non facilisis ex nisl sit amet augue. Maecenas eu enim condimentum, consectetur ligula vel, tincidunt nisl. Nam laoreet dictum volutpat. Donec at erat venenatis, ultrices lorem ac, vestibulum neque.

I.2.4 Effect of the confinement

Lorem ipsum dolor sit amet, consectetur adipiscing elit. Curabitur tortor quam, imperdiet quis facilisis sed, fringilla a quam. Cras ante odio, hendrerit ac ante nec, cursus imperdiet urna. Mauris convallis ultricies purus, nec condimentum erat bibendum vel. Aliquam erat volutpat. Pellentesque condimentum, eros a consequat accumsan, turpis sem euismod nisi, sed fringilla quam turpis sit amet erat. Mauris dictum odio sed nisi dapibus, et molestie mauris rutrum. Praesent convallis dolor in nibh blandit bibendum. Quisque sit amet arcu consectetur lorem luctus venenatis nec quis dui. Aliquam erat volutpat. Aenean auctor elit nec tristique dignissim. Nulla massa mi, efficitur semper ex id, pretium eleifend massa. Vivamus sit amet orci scelerisque, gravida est ut, vulputate odio.

Curabitur eget ipsum egestas dui viverra suscipit. Cras aliquet lacus vitae erat finibus semper. Nulla pharetra eget urna vitae sodales. Nunc faucibus velit lacus, nec ornare eros aliquet quis. Donec a orci nec sem pulvinar ultricies sit amet ut arcu. Nullam id vehicula enim, at tincidunt velit. Duis vestibulum lorem a molestie fringilla. Nullam tincidunt semper placerat. Donec nibh sem, ornare eget cursus ac, luctus sit amet eros. Phasellus eget interdum nisi. Donec mollis risus id lectus fringilla, et commodo risus iaculis. Donec at lacus sed nibh posuere posuere sit amet eget sapien. In dignissim, enim sit amet convallis fermentum, lacus nulla gravida tortor, non facilisis ex nisl sit amet augue. Maecenas eu enim condimentum, consectetur ligula vel, tincidunt nisl. Nam laoreet dictum volutpat. Donec at erat venenatis, ultrices lorem ac, vestibulum neque.

I.3 Fine and hyperfine structure of a magnetic atom in II-VI semiconductor

I.3.1 Mn atom in II-VI semiconductor

Mn in a lattice -> modification of orbital -> spin-orbit interaction. Magnetic anisotropy + anisotropy of strain. (Mn has nuclear spin 5/2 -> hyperfine interaction?)

Figure I.4: Mn in Zinc-Blend lattice

Lorem ipsum dolor sit amet, consectetur adipiscing elit. Curabitur tortor quam, imperdiet quis facilisis sed, fringilla a quam. Cras ante odio, hendrerit ac ante nec, cursus imperdiet urna. Mauris convallis ultricies purus, nec condimentum erat bibendum vel. Aliquam erat volutpat. Pellentesque condimentum, eros a consequat accumsan, turpis sem euismod nisi, sed fringilla quam turpis sit amet erat. Mauris dictum odio sed nisi dapibus, et molestie mauris rutrum. Praesent convallis dolor in nibh blandit bibendum. Quisque sit amet arcu consectetur lorem luctus venenatis nec quis dui. Aliquam erat volutpat. Aenean auctor elit nec tristique dignissim. Nulla massa mi, efficitur semper ex id, pretium eleifend massa. Vivamus sit amet orci scelerisque, gravida est ut, vulputate odio.

Curabitur eget ipsum egestas dui viverra suscipit. Cras aliquet lacus vitae erat finibus semper. Nulla pharetra eget urna vitae sodales. Nunc faucibus velit lacus, nec ornare eros aliquet quis. Donec a orci nec sem pulvinar ultricies sit amet ut arcu. Nullam id vehicula enim, at tincidunt velit. Duis vestibulum lorem a molestie fringilla. Nullam tincidunt semper placerat. Donec nibh sem, ornare eget cursus ac, luctus sit amet eros. Phasellus eget interdum nisi. Donec mollis

Figure I.5: Mn fine and hyperfine structure

risus id lectus fringilla, et commodo risus iaculis. Donec at lacus sed nibh posuere posuere sit amet eget sapien. In dignissim, enim sit amet convallis fermentum, lacus nulla gravida tortor, non facilisis ex nisl sit amet augue. Maecenas eu enim condimentum, consectetur ligula vel, tincidunt nisl. Nam laoreet dictum volutpat. Donec at erat venenatis, ultrices lorem ac, vestibulum neque.

I.3.2 Cr atom in II-VI semiconductor

Figure I.6: Cr in Zinc-Blend lattice

Lorem ipsum dolor sit amet, consectetur adipiscing elit. Curabitur tortor quam, imperdiet quis facilisis sed, fringilla a quam. Cras ante odio, hendrerit ac ante nec, cursus imperdiet urna. Mauris convallis ultricies purus, nec condimentum erat bibendum vel. Aliquam erat volutpat. Pellentesque condimentum, eros a consequat accumsan, turpis sem euismod nisi, sed fringilla quam turpis sit amet erat. Mauris dictum odio sed nisi dapibus, et molestie mauris rutrum. Praesent convallis dolor in nibh blandit bibendum. Quisque sit amet arcu consectetur lorem luctus venenatis nec quis dui. Aliquam erat volutpat. Aenean auctor elit nec tristique dignissim. Nulla massa mi, efficitur semper ex id, pretium eleifend massa. Vivamus sit amet orci scelerisque, gravida est ut, vulputate odio.

Figure I.7: Atomic configuration in Jahn-Teller effect + three minima

Curabitur eget ipsum egestas dui viverra suscipit. Cras aliquet lacus vitae erat finibus semper. Nulla pharetra eget urna vitae sodales. Nunc faucibus velit lacus, nec ornare eros aliquet quis. Donec a orci nec sem pulvinar ultricies sit amet ut arcu. Nullam id vehicula enim, at tincidunt velit. Duis vestibulum lorem a molestie fringilla. Nullam tincidunt semper placerat. Donec nibh sem, ornare eget cursus ac, luctus sit amet eros. Phasellus eget interdum nisi. Donec mollis risus id lectus fringilla, et commodo risus iaculis. Donec at lacus sed nibh posuere posuere sit amet eget sapien. In dignissim, enim sit amet convallis fermentum, lacus nulla gravida tortor, non facilisis ex nisl sit amet augue. Maecenas eu enim condimentum, consectetur ligula vel, tincidunt nisl. Nam laoreet dictum volutpat. Donec at erat venenatis, ultrices lorem ac, vestibulum neque.

Figure I.8: Degeneracy breaking under Jahn-Teller effect

Figure I.9: Strain effect on ground state + degeneracy breaking by this symetry reduction

I.4 A simple example: the X-Mn system

Lorem ipsum dolor sit amet, consectetur adipiscing elit. Curabitur tortor quam, imperdiet quis facilisis sed, fringilla a quam. Cras ante odio, hendrerit ac ante nec, cursus imperdiet urna. Mauris convallis ultricies purus, nec condimentum erat bibendum vel. Aliquam erat volutpat. Pellentesque condimentum, eros a consequat accumsan, turpis sem euismod nisi, sed fringilla quam turpis sit amet erat. Mauris dictum odio sed nisi dapibus, et molestie mauris rutrum. Praesent

Figure I.10: Overall energy structure (with +/- 2 which doesn't luminesce)

convallis dolor in nibh blandit bibendum. Quisque sit amet arcu consectetur lorem luctus venenatis nec quis dui. Aliquam erat volutpat. Aenean auctor elit nec tristique dignissim. Nulla massa mi, efficitur semper ex id, pretium eleifend massa. Vivamus sit amet orci scelerisque, gravida est ut, vulputate odio.

Figure I.11: QD spectra 0 Mn, 1 Mn, 2 Mn

Curabitur eget ipsum egestas dui viverra suscipit. Cras aliquet lacus vitae erat finibus semper. Nulla pharetra eget urna vitae sodales. Nunc faucibus velit lacus, nec ornare eros aliquet quis. Donec a orci nec sem pulvinar ultricies sit amet ut arcu. Nullam id vehicula enim, at tincidunt velit. Duis vestibulum lorem

a molestie fringilla. Nullam tincidunt semper placerat. Donec nibh sem, ornare eget cursus ac, luctus sit amet eros. Phasellus eget interdum nisi. Donec mollis risus id lectus fringilla, et commodo risus iaculis. Donec at lacus sed nibh posuere posuere sit amet eget sapien. In dignissim, enim sit amet convallis fermentum, lacus nulla gravida tortor, non facilisis ex nisl sit amet augue. Maecenas eu enim condimentum, consectetur ligula vel, tincidunt nisl. Nam laoreet dictum volutpat. Donec at erat venenatis, ultrices lorem ac, vestibulum neque.

Figure I.12: Mn energy level in a QD

Bibliography

[1] E. O. Kane, "Band structure of indium antimonide", Journal of Physics and Chemistry of Solids **1**, 249–261 (1957).

[2] C. Le Gall, "Dynamics and Optical contrôl of a single spin in a Quantum Dot", Theses (Université de Grenoble, Nov. 2011).

[3] J. M. Luttinger, "Quantum theory of cyclotron resonance in semiconductors: general theory", Phys. Rev. **102**, 1030–1041 (1956).

[4] G. Bir and G. Pikus, *Symmetry and strain-induced effects in semiconductors*, Wiley (1974).

[5] J. Allègre, B. Gil, J. Calatayud, and H. Mathieu, "Deformation potentials of cdte epilayers from piezo and wavelength modulation reflectivity spectra analysis", Journal of Crystal Growth **101**, 603–607 (1990).

[6] J. M. Luttinger and W. Kohn, "Motion of electrons and holes in perturbed periodic fields", Phys. Rev. **97**, 869–883 (1955).

[7] J.-L. Basdevant and J. Dalibart, "Mécanique quantique", in (Les éditions de l'École Polytechnique, 2002) Chap. 2, p. 80.